Essential Readings in Light Metals: Cast Shop for Aluminum Production.
Edited by John F. Grandfield and Dmitry G. Eskin.

3. OXIDATION AND DROSS PROCESSING

The formation of aluminum oxide and dross is an unavoidable issue in cast house processing. It remains one of the most important challenges from economic, quality, and environmental perspectives. Thus, we have listed important papers on the fundamentals of oxide formation. We also have included papers on dross processing in which the aim is to maximize recovery of metal values.

Essential Readings in Light Metals: Cast Shop for Aluminum Production.
Edited by John F. Grandfield and Dmitry G. Eskin.

Light Metals — From *Light Metals 1989*, Paul G. Campbell, Editor

OXIDATION OF LIQUID ALUMINUM - MAGNESIUM ALLOYS

M.P. Silva and D.E.J. Talbot

Department of Materials Technology
Brunel, The University of West London
Uxbridge, Middx. UB8 3PH, England.

The isothermal oxidation of liquid binary aluminum alloys with 1-9 wt-% magnesium was studied thermogravimetrically for temperatures in ranges extending from their solidus temperatures to 725°C. For all of these compositions, the most stable chemcal species is MgO and this was the only oxide component detected by X-ray, EDX and electron diffraction techniques. The initial oxide film formed on the clean liquid metal substrate was amorphous and highly protective, restricting the oxidation rate. After an incubation period of 1-2 hr., depending on the magnesium content of the metal, the oxidation accelerated abruptly, an event assoicated with the onset of crystallisation. The effects are attributed to (i) structural characteristics of amorphous MgO and (ii) disruption of the original protective oxide film by stresses induced by the growth of crystalline MgO nucleated within the amorphous layer. Within the solidus/liquidus temperature range, the oxide film was crystalline throughout the oxidation period and oxidation was rapid ab initio.

INTRODUCTION

The oxidation of liquid aluminum-magnesium alloys is of economic interest because selective loss of magnesium occurs during industrial melting operations.

Previous investigations (1-5) have yielded results which suggest inter alia that the spinel, $MgAl_2O_4$, is a normal component of the oxide formed on aluminum-magnesium alloys and that its formation after an incubation period is the stimulus for breakaway oxidation which leads to the develoment of swollen black films (2,3). The validity of these ideas is uncertain since they are based on results from experimental approaches subject to error from e.g.:

(i) The use of thermogravimetric equipment with insufficient sensitivity to identify important features which might occur early in the oxidation process.

(ii) Departure from truly isothermal conditions, so that the progress of oxidation is conditioned by oxide films formed before the metal is completely liquid.

(iii) Serious depletion of the nominal magnesium content by selective oxidation.

The purpose of the present work was to obtain new results using strictly controlled experimental conditions to provide a more secure basis from which to extract some of the fundamental principles which apply.

EXPERIMENTAL

Materials

Alloys with the analyses given Table I were chill-cast into moulds 8cm x 8cm x 30cm. Longitudinal sections were cut from the ingots, avoiding zones susceptible to surface macro-segregation or central unsoundness, and machined to 2cm diameter bars. The bars were heat-treated for 48hr. at 50-150°C below the equilibrium solidus temperatures to disperse micro-segregation. This provided the stock from which samples for the experiments were taken.

Table I Analyses of Experimental Materials

wt-%

Nominal Mg	Mg	Fe	Si	Cu	Zn, Ti, Cr Mn, Na
1	1.3	0.004	0.002	0.004	<0.001
3	3.1	0.005	0.003	0.003	<0.001
5	5.1	0.006	0.003	0.005	<0.001
7	7.4	0.003	0.002	0.006	<0.001
9	9.3	0.004	0.004	0.004	<0.001

Thermogravimetric Measurements

The thermogravimetric measurements were made using a Sartorius Model 4410 automatic recording vacuum microbalance, with a sensitivity of 1μg, arranged to monitor continuously the mass of a liquid sample contained in an alumina crucible suspended from the balance beam by a silica filament. The balance beam and the suspended crucible and sample were enclosed in a system capable of maintaining a high vacuum indefinitely, thus permitting very precise control of the atmosphere. The balance system was provided with access to a mercury diffusion vacuum pump capable of reducing the pressure to $<10^{-5}$ Pa and to gas trains to provide any required atmosphere. The sample was heated by an external furnace. The assembly is illustrated schematically in Figure 1.

Every sample was prepared in the form of a machined disc 16mm diameter x 6mm thick. These dimensions were chosen so that the sample fitted closely inside the crucible when placed flat, thereby minimising disturbance to the metal during melting. Immediately before use, the sample was abraded on 600 grade emery paper, etched in 2.5 M sodium hydroxide solution, rinsed in water and ethanol and dried.

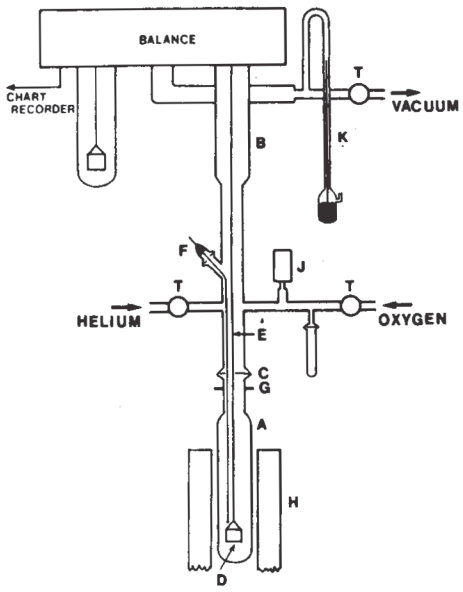

Figure 1 Thermogravimetric Equipment

A Sample chamber
B Microbalance tube
C Vacuum-tight joint
D Alumina crucible & sample
E Silica suspension
F Thermocouple
G Radiation shield
H Furnace
J Vacuum gauge
K Manometer
T Taps

Sensitive thermobalances are susceptible to instability due to convection currents which cause least interference if the density of the atmosphere is low. To minimise the effect, the sample was oxidised not in air but in an oxygen/helium mixture with the same proportion of oxygen, i.e. 0.21. The atmosphere was dried to a dew point of 90K.

In developing a suitable experimental procedure, the over-riding considerations were to prevent premature oxidation below the test temperature and to suppress magnesium evaporation before commencing a test. These requirements were met as follows. A sample was heated and its temperature stabilised at the prescribed value in the helium fraction. The helium was 99.999% pure as certified by the suppliers. Before admitting it, the system contianing the sample was evacuated to a pressure of $<10^{-5}$ Pa. The criterion to proceed was that no change in mass could be detected when the sample was held indefinitely in helium at the test temperature. Oxidation was initiated by admitting the oxygen fraction to form the mixture.

The definition of the surface area of the liquid sample exposed to oxidation requires some comment. After oxidation, the whole of the cylindrical surface of the sample had retracted away from the sides of the crucible under the influence of surface tension and exhibited oxidation products similar to those observed on the upper circular surface. Some lesser oxidation occurred on the lower circular face, indicating some restricted access of oxygen. At some temperatures in the solidus/liquidus range, the samples were sufficiently rigid to permit a comparison between the masses of oxide formed in measurements with samples laid flat in the crucible and in corresponding measurements with the sample standing on edge. This established that the effective area of the lower face was 0.25 of its geometric area. The area available for oxidation was therefore taken as $\pi(1.25r^2 + 2\pi rh)$.

Thermogravimetric measurements were made for all of the alloys at intervals of 25°C at temperatures in ranges extending from the solidus temperatures to 725°C (6). The period of oxidation was limited to 2 hours to avoid significantly depleting the magnesium content below the nominal composition. Replicate measurements were made for shorter periods to provide a systematic series of oxidised surfaces for every alloy for use in analysing the evolution of the oxide systems.

Characterisation of Oxidation Products

The evolution of oxide topographies was examined by scanning electron microscopy of sample surfaces. Flakes of oxide were detached from the sample surfaces for examination by X-ray diffraction and by a STEM system with electron diffraction and EDX facilities to provide phase identification, local area analysis and information on the crystal and lattice structures.

RESULTS

For brevity, only selected results sufficient to establish the essential features of oxidation are given.

Figures 2 to 4 give the thermogravimetric results for alloys with 3, 5 and 7% magnesium. The results for alloys with 1 and 9% magnesium were broadly similar to those for 3 and 7% magnesium respectively.

Figures 6 and 7 give TEM micrographs and electron diffraction patterns for oxides formed on the alloys with 3% and 5% magnesium in the liquid state.

Oxidation of Liquid Metal

Liquid metal exhibited one of two oxidation modes:

Mode A: Oxidation diminishing progressively throughout the whole period, characteristic of a coherent protective oxide exercising diffusion control.

Mode B: Oxidation diminishing at first but accelerating rapidly after an incubation period, characteristic of an oxide which is initially coherent and protective but which later either undergoes structural change or loses its coherency, leading to breakaway.

The alloys with 3% magnesium or less exhibited mode A oxidation and the alloys with 5% magnesium or more exhibited mode B. Figures 3 and 4 show that the incubation period diminished for increased temperature and for increased magnesium content.

Oxidation of Partially Liquid Metal

For temperatures within the solidus/liquidus range, oxidation proceeded rapidly from the beginning and no subsequent breakaway was observed, as apparent in Figures 2 to 4.

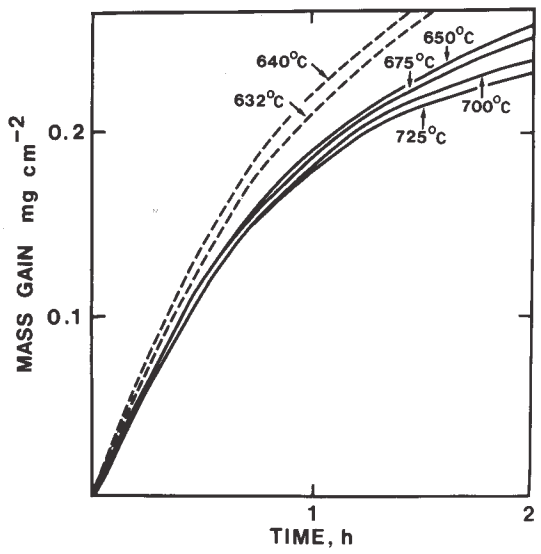

Figure 2 Mass gain v. time for Al - 3% Mg alloy

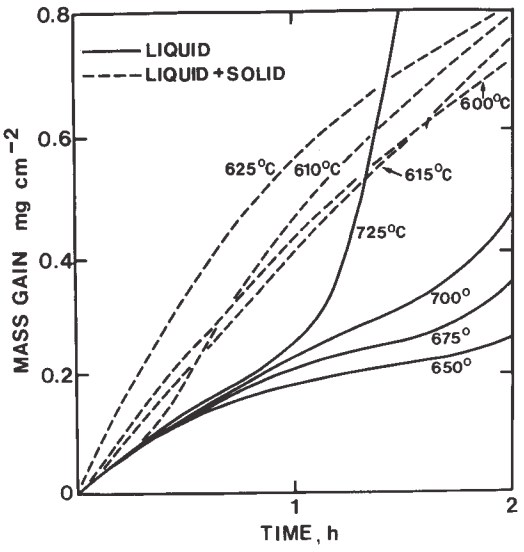

Figure 3 Mass gain v. time for Al - 5% Mg alloy

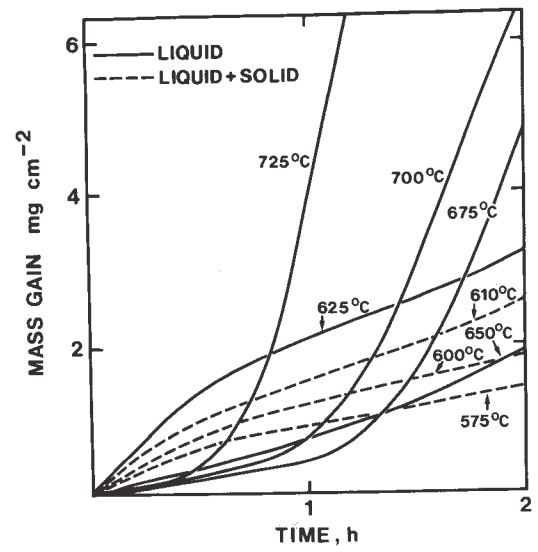

Figure 4 Mass gain v. time for Al - 7% Mg alloy

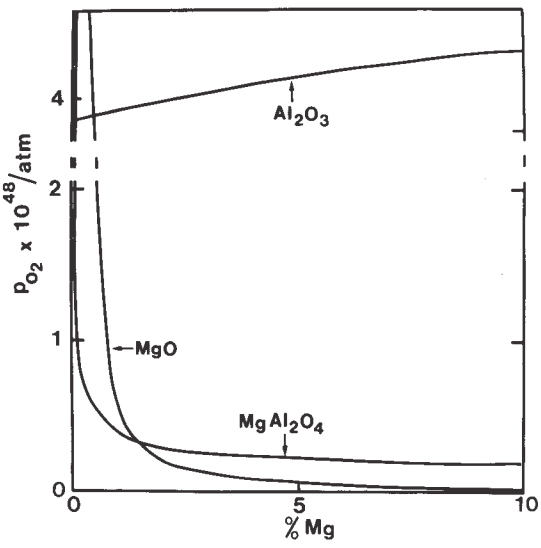

Figure 5 Oxygen pressures for formation of oxides

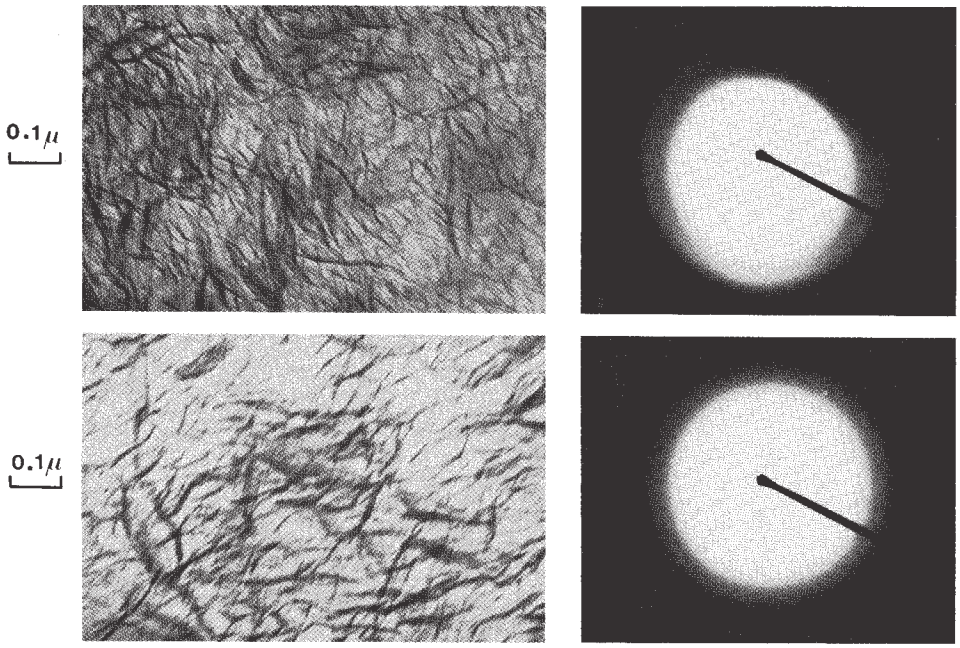

Figure 6 TEM Micrographs and corresponding electron diffraction patterns from oxide formed on aluminum - 3% magnesium alloy at 700°C. a) and b) after 0.5 hr. c) and d) after 2 hr.

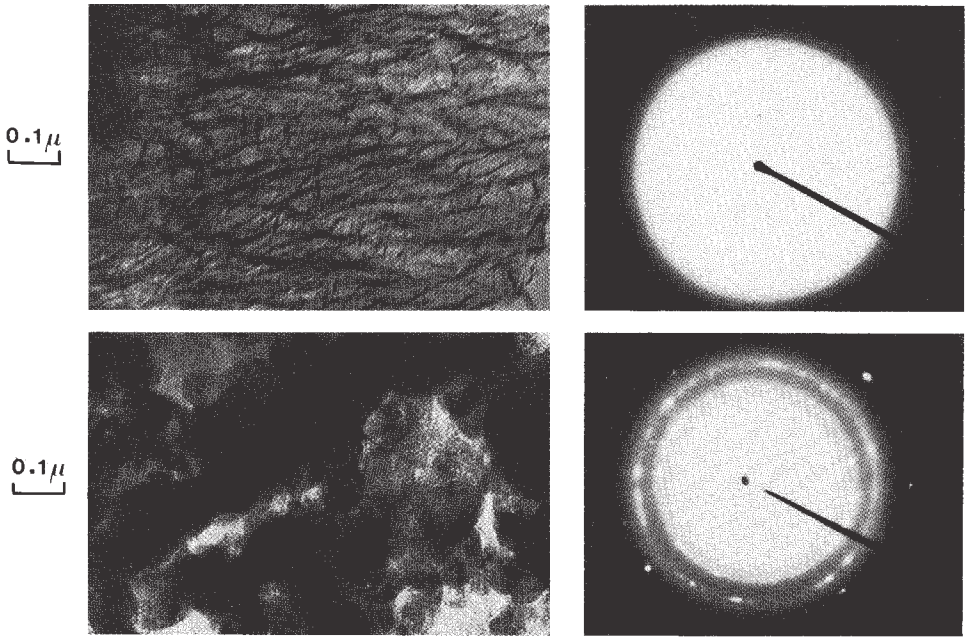

Figure 7 TEM Micrographs and corresponding electron diffraction patterns from oxide formed on aluminum - 5% magnesium alloy at 650°C. a) and b) after 0.5 hr. c) and d) after 2 hr.

DISCUSSION

Stability of Oxidation Products

The standard Gibbs free energy of formation for oxides in the aluminum-magnesium-oxygen system are:

$$2Mg(l) + O_2(g) = 2MgO(s)$$

$$\Delta G^\circ = -1215126 - 2T \log T + 225.3\ T\ J\ mol^{-1} \quad (1)$$

$$4/3\ Al(l) + O_2(g) = 2/3\ Al_2O_3(s)$$

$$\Delta G^\circ = -1130718 - 10.5\ T \log T + 257\ T\ J\ mol^{-1} \quad (2)$$

$$\tfrac{1}{2}Mg(l) + Al(l) + O_2(g) = \tfrac{1}{2}\ MgAl_2O_4(s)$$

$$\Delta G^\circ = 1169585 - 8.4T \log T + 245.6\ T\ J\ mol^{-1} \quad (3)$$

Equations (1) and (2) for MgO and Al_2O_3 are those given by Kubaschewski and Alcock (7). Equation (3) for $MgAl_2O_4$ is not available explicitly and has been obtained by summing the standard enthalpies and entropies of the reactants and products also given by Kubaschewski and Alcock (7), making the reasonable assumption that the enthalpy and entropy of formation for $MgAl_2O_4$ is not significantly temperature-dependant.

The relative stabilities of the oxides as functions of magnesium content for the alloys were determined in the usual way by comparing the notional equilibrium oxygen pressures calculated using Equations (1)-(3) and values given by Bhatt and Garg (8) for the activity coefficients of magnesium and aluminum in the liquid binary system. Some results of calculations for 725°C are given as an example in Figure 5. Figure 5 shows that for magnesium contents above 1.5 wt-% the most stable oxide is MgO since it is in equilibrium with the lowest oxygen pressure. For magnesium contents in the range 0.02-1.5 wt-% the most stable oxide is $MgAl_2O_4$.

Oxidation Products Formed on Liquid Metal

The only oxide found on any of the oxidised samples was the stable chemical species MgO. Strictly, the aluminum - 1.3% magnesium alloy lies just inside the composition range where $MgAl_2O_4$ is the thermodynamically stable oxide but by analogy with the iron-chromium system, nucleation of the complex spinel structure at the metal surface is probably difficult (9). The MgO was found in both crystalline and amorphous forms. The identity of the crystalline form was established by comparing interplanar spacings derived from X-ray diffraction spectra with standard values given in the ASTM powder diffraction data files and by matching electron diffraction patterns with patterns derived from known oxides. The amorphous form could be identified only by recourse to elemental analysis using the STEM/EDX facility.

Simple calculation shows that the oxide/metal volume ratio for the formation of MgO on the liquid binary aluminum-magnesium alloys is close to unity, i.e. favorable for the production of a protective film.

The MgO oxide film was indeed protective throughout the oxidation period for the liquid alloys exhibiting mode A oxidation and also during the initial period for the alloys exhibiting mode B oxidation. It was noteworthy that the MgO was in the amorphous form during the periods when the oxide afforded protection but transformed to the crystalline form at the onset of a breakaway. This is illustrated by the examples given in Figures 6 and 7 which show sequences of TEM micrographs and corresponding electron diffraction patterns typical of mode A and mode B oxidation respectively. For the aluminum - 3% magnesium alloy, which exhibited no breakaway, all of the electron diffraction patterns were composed of clear rings characteristic of an amorphous material. For the aluminum - 5% magnesium alloy, the progressive resolution of the electron diffraction rings into spots and evidence of a developing grain structure in the corresponding TEM micrographs mark the onset of crystallisation, which correlates with the breakaway evident in Figure 3.

It is not surprising that the initial oxide formed on a clean liquid metal surface should be amorphous, since the mobile random structure of the substrate can have no directive influence on the structure forming upon it. Amorphous MgO is expected to afford greater protection than its crystalline counterpart. MgO is an extrinsic oxide in which the mobile ionic species controlling oxide growth is Mg^{2+}. It is well known that for amorphous materials generally charge carriers have lower mobility than in the corresponding crystalline materials because they are bound to localised energy states which exist within the mobility gap due to the disorder in the material (10-11). The effect is to reduce the mobility of Mg^{2+} ions by increasing the activation anergy for the electron flow needed to preserve electroneutrality. A further factor limiting the mobility of a diffusing species in an amorphous material is the absence of preferred diffusion paths in grain boundaries.

Amorphous MgO is, of course, unstable with respect to the crystalline material and given time and opportunity will transform by nucleation and growth of crystals. This, of course, explains the incubation period, since as Figures 5 and 6 show, the onset of breakaway oxidation is synchronised with the onset of crystallisation. The crystal growth which occurs is the progenitor of several effects which destroy the protection afforded by the amorphous material, i.e.:

(i) The mobility of Mg^{2+} ions is increased

(ii) Structural defects, e.g. grain boundaries are generated, offering preferred diffusion paths

(iii) Growth stresses promote mechanical disruption of the original protective film leading to irregular growth of subsequent oxide, as was in fact observed.

Oxidation Products Formed on Partially Liquid Metal

The work described is only part of an extensive investigation on the oxidation of aluminum-magnesium alloys generally, which will be fully reported in due course. In particular, full presentation and discussion of the results obtained for metal oxidised in the partially liquid state is outside of the scope of the present paper. Nevertheless, the character of the oxidation observed for the alloys in this condition is so different from that of the same alloys when oxidised in the completely liquid state that some reference to it is essential.

In the partially liquid state, oxidation was rapid from the very early stages. This is explained by evidence of electron diffraction patterns from the oxidation products (not illustrated), which showed that the MgO was produced in and remained in the crystalline form. Thus, the initial protection afforded by a film

of amorphous MgO, characteristic of the completely liquid metal was omitted. A corollary is that no process analogeous to the crystallisation of the amorphous film was possible, so that the mass gain/time relationship exhibited no early breakaway phenomenon.

Metal in the partially liquid state contains a proportion of solid metal, whose ordered lattice structure can stimulate epitaxial nucleation of crystal nuclei, thus seeding the oxide growing over the liquid fraction, promoting instant crystallisation.

Some Implications

The foregoing discussion illustrates some of the difficulties in applying experimental results to the task of minimising oxidative losses in industrial melting operations.

The present results accord with some well-established principles, e.g. that the mass of oxide formed on liquid metal increases with increasing magnesium content, temperature and time of exposure.

It may be unexpected to assert that the oxide film formed on the clean surface of liquid aluminium-magnesium alloys is protective, and remains so at low temperatures for an hour or two before the onset of very rapid oxidation. Perhaps there is a case for reviewing holding and skimming schedules to restrict the make of dross.

Oxidation in the temperature range between the solidus and liquidus temperatures is obviously a major contributor to the mass of oxide formed on melting. This, of course, is well known from experience and is countered in practice by e.g. submerging scrap to be melted beneath the surface of molten metal.

REFERENCES

1. N. Cochran, L. Belitskus and L. Kinosz, Met. Trans., (B) 8 (1977), 323.

2. S. Balicki, Prace. Inst. Hutniczych., 10 (1958), 208.

3. W. Theile, Aluminium, 38 (1962), 780.

4. L. Belitskus, Oxid. Metals, 8 (1974) 303.

5. I. Haginoya and T. Fukusako, J. Japan Inst. Light Met., 24 (1974), 364.

6. G.V. Raynor, "Annotated Equilibrium Diagram Series", Inst. Metals, (1945), No. 5.

7. O. Kubaschewski and C.B. Alcock, "Metallurgical Thermochemistry", (1979), New York, Pergamon Press.

8. B. Bhatt and S. Garg, Met. Trans., (B) 7 (1976) 271.

9. O. Kubaschewski and E. Hopkins, "Oxidation of Metals and Alloys", (1967), London, Butterworths.

10. N. Mott and A. Davis, "Electronic Processes in Non-Crystalline Materials", (1979), Oxford, Clarendon Pres.

11. R. Chittick, J. Non-Cryst. Solids, 3 (1970), 255.